Hindawi
Scientific Programming
Volume 2022, Article ID 9336561, 13 pages
https://doi.org/10.1155/2022/9336561

Research Article

Intelligent Control Strategy of Electrohydraulic Drive System for Raising Boring Power Head

Jun Zhang,[1,2,3] **Qinghua Liu**,[1,3] **Yun Chen**,[1,3] **Jiguo Wang**,[1,3] **Jinpu Feng**,[1,3] **Qingliang Meng**,[1,3] **Wei Cao**,[1,3] **Wei Tu**,[1,3] **and Xiaohui Gao**[4]

[1]*Ningxia Tiandi Benniu Industry Group Co., Ltd., Shizuishan 750000, China*
[2]*School of Mechanical and Transportation Engineering, Taiyuan University of Technology, Taiyuan 030024, China*
[3]*China Coal Science and Industry Group Co., Ltd., Beijing 100013, China*
[4]*School of Mechanical Engineering, Taiyuan University of Science and Technology, Taiyuan 030024, China*

Correspondence should be addressed to Jun Zhang; zhangjun07@tyut.edu.cn

Received 11 May 2022; Revised 5 June 2022; Accepted 15 June 2022; Published 15 July 2022

Academic Editor: Lianhui Li

The power head is the key part of the rock breaking work of the raise boring machine. Because the power head cannot adjust speed in time with the change in complex rock stratum, it leads to high failure rate, low work efficiency, and even accidents, so it is urgent to improve the controllability of the power head. In this paper, the electrohydraulic coupling mathematical model of the power head is established using the characteristic equations of dynamics and hydraulic components, and the control strategy of the fractional electrohydraulic drive system of the power head is proposed; genetic algorithm (GA), particle swarm optimization (PSO), and whale optimization algorithm (WOA) are used to adjust the parameters of FOPID, so as to improve the control effect of electrohydraulic system. The results show that the step response of WOA-FOPID control strategy is also better than that of genetic algorithm (GA) and particle swarm optimization (PSO). It can reach a stable state in 0.02 seconds, and the overshoot is only 0.12137%. The test verifies the correctness of the adaptive control and simulation results of the power head, which can effectively improve the adaptability of the power head to complex coal seams.

1. Introduction

Due to the advantages of the high safety, relatively low cost, and ensuring the safety of operators to the greatest extent, the reverse well drilling rig is widely used in underground roadway space, mine development, subway tunnel, and other projects, and the drilling technology is also a fundamental change technology for well hole drilling. In recent years, with the improvement of intelligent control technology of the drive system of the reverse well drilling rig, it has not only accelerated the speed of excavation but also greatly alleviated the labor intensity.

The power head is the key component of the reverse well drilling rig, and its control method and effect directly affect the safety and stability of the reverse well drilling rig in construction. At the same time, the intelligent control of the power head also has a positive role in promoting the intelligent construction of coal mines nationwide. Therefore, the intelligent control strategy of the electrohydraulic drive system of the power head has attracted the attention of the majority of scientific researchers at home and abroad. For example, Wang and Yang [1], and others studied the relationship between the four parameters of drill pipe tension, torque, rotational speed, and drilling speed in the power head control system. Shen and Liu [2] formulated the mathematical modeling and robust integral adaptive controller of the power head valve-controlled hydraulic motor based on Padde's theorem and the reverse step derivation method, which improved the accuracy and tracking speed of the system control. Yang [3] proposed a fuzzy PID control algorithm based on the problem of synchronization of four hydraulic motors in the power head device, which improved the synchronization accuracy of the motor. Cheng [4] used Amesim and MATLAB-Simulink to construct a joint

simulation model of the test bench drilling simulation system, and Cheng Lilin designed a fuzzy adaptive PID controller to analyze the control performance of the power head system. Zhang [5] used the method of co-simulation between Amesim and MATLAB-Simulink, the adaptability of different control algorithms of traditional PID fuzzy and feedback linear synovial membrane structure to the position tracking control of valve-controlled asymmetrical hydraulic cylinders is analyzed, and the problems of nonlinearity and low control accuracy of the electrohydraulic control system of the power head are solved. Foreign hydraulically driven reverse well drilling rig, power head drive using electrohydraulic proportional PID control technology, control unit using PLC or engineering controller [6–9], due to the introduction of computer control technology, and a variety of more complex control logic and PID control algorithms can be realized. The above literature research has made certain contributions to the intelligent control of the electrohydraulic drive system of the power head of the reverse well drilling rig and laid a certain foundation for the intelligent control algorithm of the power head. However, the research in the above articles is based on the traditional PID control algorithm. Especially in downhole operation, complex uncertainties such as surrounding rock parameters and downhole force of the drill will make the driving head of the drill unable to adjust the control parameters in time, resulting in low drilling efficiency, short service life of rock breaking hob, and even damage to the drill bit, sticking, etc. Under special working conditions, the traditional PID control effect is not ideal, even if the PID is re-parameter tuned, it still cannot achieve a good control effect, and it is essentially impossible to overcome the shortcomings of traditional PID control technology. Therefore, the complex system has a low control accuracy, reflecting the poor sensitivity and other issues, and it is difficult to explore the intelligent control principle of the electrohydraulic drive system of the power head from a deep level, and the parameter selection of the PID controller has a great impact on the control effect, the traditional parameter tuning method is still based on experience, and it is difficult to find a set of parameters with good control effect in a short period of time.

The fractional order FOPID controller has 5-bit adjustable parameters. Compared with other control laws, it has better dynamic performance, parameter adjustment flexibility, and control accuracy [10–12], and there is a great vacancy in the research and application of fractional order FOPID in the research of electrohydraulic system control method of raising boring. Based on the internal control principle of the reaming operation of the power head of the reverse well drilling rig, if the control effect is required to have good timeliness and reliability, the parameter adjustment research of the intelligent control algorithm is also indispensable, such as the particle swarm algorithm [13–15], the genetic algorithm [16], the gravity search algorithm [17], the neural network algorithm [18], the ILMI algorithm [19], and the whale optimization algorithm [20], which are all applied in the PID controller, improving the control effect of the traditional PID controller. The method of parameter tuning that relies on experience is got ridden.

Based on this, this paper establishes the electrohydraulic coupling model of the power head of raise boring machine from the dynamic principle, electrohydraulic coupling properties, and the characteristic equation of hydraulic components and puts forward the control method of the power head electrohydraulic drive system based on fractional FOPID. To further improve the control effect of the system, the genetic algorithm (GA), particle swarm algorithm (PSO), whale optimization algorithm (WOA), three groups of intelligent optimization algorithms are used to adjust the FOPID and PID controller parameters, and the influence of the above different combination algorithms on the control system is evaluated, to provide theoretical guidance for the reliability of the reaming operation of the reverse well drilling rig [21–24]. Finally, field experiments were conducted in Liuqiao Town, Suixi County, Anhui Province, to prove the effectiveness of WOA-FOPID control strategy in electrohydraulic drive control system. It further provides new theoretical guidance for the intelligent control strategy of the electrohydraulic drive system of the power head.

2. Mathematical Modeling

This article takes a deep well lane full-section test drilling rig (raising boring) as an example to study, which is the most widely used [25] and belongs to the lower lead upward expansion type. In order to apply intelligent drilling technology to raise boring machine, taking the power head as the research object, PLC and HMI are used to design the rock breaking control system. Four variable displacement piston pumps a11vlo130lrd are connected in series into two groups, which are driven by 132 kw motors to drive four mcr15a1500w80z32a0m2l4 2S 506u two-speed radial piston motors, and the hydraulic motor also controls the rotation of the power head [26, 27]. The overall idea of the structure composition, construction process, and control scheme of the reverse well drilling rig and the power head is shown in Figure 1.

To facilitate the theoretical modeling and analysis, the basic assumptions of hydraulic motor modeling are made. On this basis, the proportional amplifier, electrohydraulic proportional control valve, power head electrohydraulic coupling model, and the transfer function of power head hydraulic motor speed are established, respectively. The signal output by the controller is a voltage signal or a current signal, which is a component that amplifies its input signal and simplifies this model to a proportional link because of its input and output characteristics. Its transfer function is as follows:

$$G_i = \frac{I(s)}{U_i(s)} = K_b, \tag{1}$$

where K_b is the gain of the proportional amplifier.

The current signal output by the proportional link is based on dynamics and electromagnetic induction to drive the proportional solenoid movement, and then, the valve spool generates motion, thereby controlling the size of the

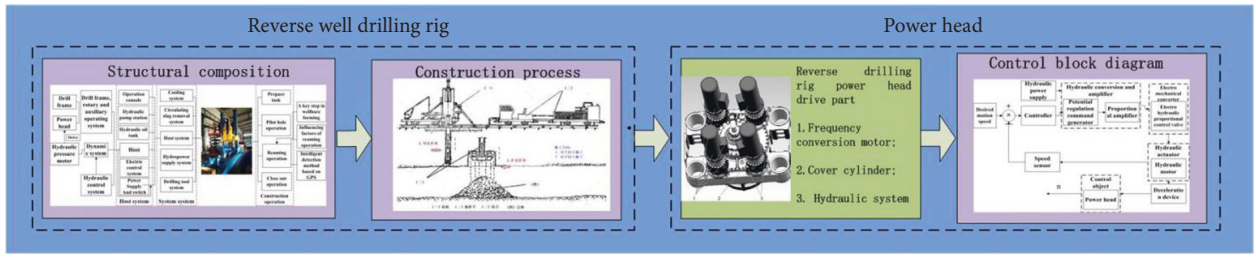

Figure 1: Overall train of thought block diagram.

valve opening and the direction of the liquid in and out. The working principle of the electrohydraulic proportional control valve is established, and the following expressions are established for the relationship between the coil current in the electromagnet, the driving force of the electromagnet, and the displacement of the valve core:

$$\begin{cases} u = L\dfrac{di}{dt} + \left(R_c + r_\rho\right)i, \\ F_d(t) = K_I U(t), \\ F_M(t) = m\dfrac{d^2x}{dt^2} + c\dfrac{dx}{dt} + k_s x. \end{cases} \tag{2}$$

The transfer function obtained by pulling the change of (2) is as follows:

$$G_2 = \frac{X(s)}{I(s)} = \frac{K_{xi}}{s^2 + 2\omega_n\xi s + \omega_n^2}. \tag{3}$$

In the formula, ω_n is the natural frequency of the spool, ξ is the damping ratio of the spool, and K_{xi} is the gain of the electrohydraulic proportional valve.

The electrohydraulic coupling model of the power head is composed of the hydraulic motor connected to the power head through the deceleration device, so the following relationship is established according to the flow continuity of the hydraulic motor valve, the static characteristic equation, the dynamic balance equation of the shaft, and C_d:

$$\begin{cases} q_L = C_d A x\sqrt{\dfrac{1}{\rho}\left(p_s - p_L\right)}, \\ q_L = D_m\dfrac{d\theta_m}{dt} + C_{tm}p_L + \dfrac{V_t}{4\beta_e}\dfrac{dp_L}{dt}, \\ T = D_m P_L = J\dfrac{d^2\theta_m}{dt} + B_m\dfrac{d\theta_m}{dt} + G\theta_m + T_f, \\ T_f = \dfrac{J_e s\omega_d(s) + B_e\omega_d(s) + T_d(s)}{i}. \end{cases} \tag{4}$$

As can be seen from Figure 1, the hydraulic motor and the power head are connected through the deceleration device, and the angular velocity exists: $\overrightarrow{r}$. A pull transform on equation (4) is performed to get the following equation:

$$\begin{aligned} T &= D_m P_L(s), \\ &= \left(iJ_1 + J_e\right)s\omega_d(s) + \left(iB_m + B_e\right)\omega_d + \frac{T_d(s)}{i}. \end{aligned} \tag{5}$$

From (5), it can be known that the equivalent inertia of the power head $J_d = iJ_1 + J_e$ is equivalent to viscous damping coefficient $B_d = iB_m + B_e$. The transfer function of the electrohydraulic coupling power head model under no-load state is sorted out:

$$G_{d1}(s) = \frac{\omega_d(s)}{U_i(s)} = \frac{K_d}{\left(s^2 + 2\omega_n\xi s + \omega_n^2\right)\left(s^2/\omega_d^2 + 2\xi_d/\omega_d s + 1\right)}, \tag{6}$$

where $K_d = K_\alpha K_{xi} K_q D_m / iD_m^2 + B_d(C_{tm} + K_c)$, $\omega_d = \sqrt{\beta_e[iD_m^2 + B_d(C_{tm} + K_c)]/V_t J_d}$, and $\xi_d = J_d\beta_e(C_{tm} + K_c) + B_d V/2\sqrt{\beta_e V_t J_d[iD_m^2 + B_d(C_{tm} + K_c)]}$.

Proportional amplifier, electrohydraulic proportional valve, and hydraulic motor-related parts of the parameters are as follows: the inertia of the motor shaft J is 67 kg·m^2, $\overrightarrow{r}$ is 0.4755 kg·m^2, the total volume V_t of the connecting pipe is 3×10^{-4} m^3, the elastic modulus of the system is 6.9×10^8 N/m^2, the flow gain K_q is 2.42 m^2/s, the motor displacement is 2.39×10^{-4} m^3/rad, the gear ratio of the reducer is i of 6.817, and the open-loop transmission function of the power displacement signal by calculating the angular velocity of the power head is as follows:

$$\begin{aligned} G_{d1}(s) &= \frac{\omega_d(s)}{U_i(s)} = \frac{K_d}{\left(s^2 + 2\omega_n\xi s + \omega_n^2\right)\left(s^2/\omega_d^2 + 2\xi_d/\omega_d s + 1\right)}, \\ &= \frac{8.476\times10^4}{5.487\times10^{-5}s^4 + 0.0252s^3 + 2.85s^2 + 432.59s + 10000}. \end{aligned} \tag{7}$$

By (7), we obtain the system without interference and control Bode diagram as shown in Figure 2.

From Figure 2, it can be seen that when the amplitude-frequency characteristics reach zero decibels, the phase-frequency characteristics are below −180° line, and the phase lag point has a negative stability margin at the 180° point, so there is a stability problem in the system, but due to the stability of the system itself and the dynamic characteristics, to make the system have a stable margin, it is necessary to add a controller to adjust to meet the stability requirements.

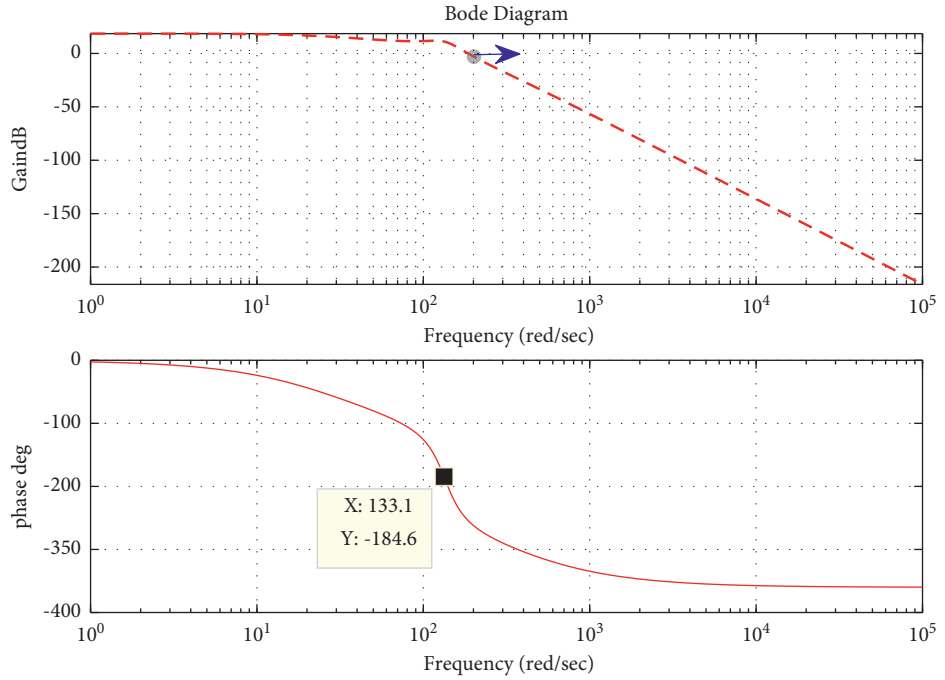

Figure 2: Open-loop Bode diagram of the system without interference and control.

3. Fractional Order FOPID Controller Design

As a branch of the control field, fractional order (FOPID) control has many advantages such as flexible and precise parameter adjustment, large system stability margin, and strong system robustness and has been widely used in different types of controller design [28–30]. Fractional order $PI^{\lambda}D^{\mu}$ control was first proposed by Igor Podlubny, and its superiority over traditional PID control was demonstrated through response analysis [28–30], [31-36]. Fractional order $PI^{\lambda}D^{\mu}$ controller of the order of parameters λ and μ can take any real number, in the $P-I-D$ plane, according to the different controller parameters to take the value; FOPID control system structure is shown in Figure 3. Compared with traditional PID control, fractional $PI^{\lambda}D^{\mu}$ control can more subtly reflect the transition process from proportional control to integral control and differential control, to achieve a control effect with higher accuracy, better stability, and stronger anti-interference ability.

The mathematical expression for the FOPID controller is as follows:

$$C(s) = \frac{U(s)}{R(s)} = K_p + \frac{K_i}{s^{\lambda}} + K_d s^{\mu}, \tag{8}$$

where K_p is the proportional gain, K_i is the integral gain, K_d is the differential gain, and λ and μ are the fractional and integral orders, respectively.

4. Whale Optimization Algorithm

Based on the advantages of fractional order PID control algorithm, this paper proposes a control strategy based on WOA-FOPID algorithm. There are many kinds of parameter tuning methods for FOPID. According to the regulation characteristics of the algorithm itself, it is mainly divided into traditional method tuning and intelligent optimization algorithm tuning, and the intelligent optimization algorithm is widely used because of its self-adaptability. In this paper, genetic algorithm (GA), particle swarm optimization (PSO), and whale optimization algorithm (WOA) are combined with FOPID control theory, respectively, and the above three intelligent optimization algorithms are used to set FOPID control parameters. The structure of intelligent control algorithm FOPID control system is shown in Figure 4.

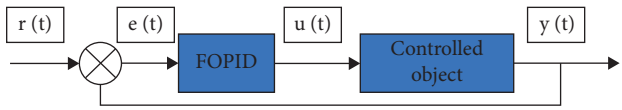

Figure 3: Structure of the FOPID control system.

To fully explore the advantages of genetic algorithm (GA), particle swarm optimization (PSO), and whale optimization algorithm (WOA), three intelligent optimization algorithms are combined with PID and FOPID, respectively, and the speed control effect of power motor is further analyzed through different control strategies. The flow chart of setting FOPID parameters by the developed intelligent optimization algorithm is shown in Figure 5.

5. Parameter Setting and Optimization Process of Real Analysis and Optimization Flow Simulation Analysis

There are many kinds of parameter tuning methods for FOPID. With the development of intelligent and control technology, according to the regulation characteristics of the algorithm itself, it is mainly divided into traditional method

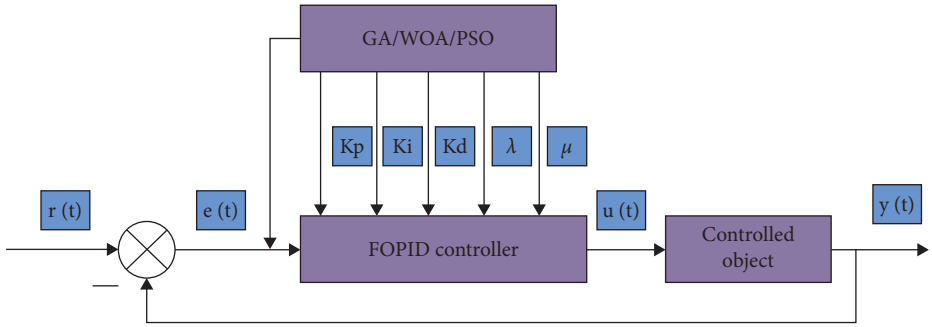

Figure 4: Structure diagram of the intelligent control algorithm FOPID control system.

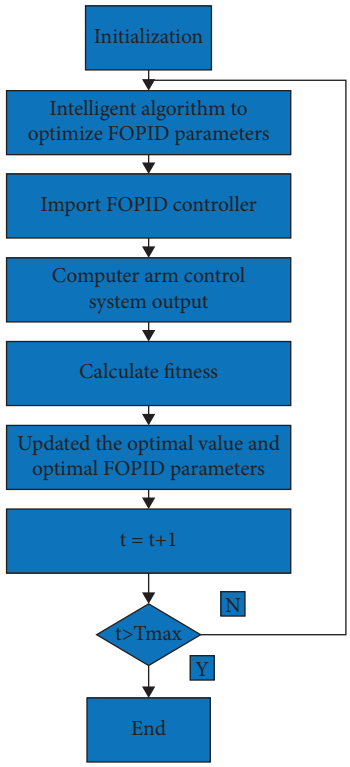

Figure 5: Flow chart of intelligent optimization algorithm for tuning FOPID parameters.

and intelligent optimization algorithm. The intelligent optimization algorithm is widely used because of its self-adaptability. The whale optimization algorithm (WOA) has been widely used because of its simple optimization mechanism and fast solution speed. The algorithm searches for the optimal solution by simulating the predation behavior of humpback whales [37–39] and solves the D-dimensional optimization problem in which f(x) is the optimization objective function:

$$Min\, f(x), s.t. 1 \le x \le u. \tag{9}$$

In servo control, the ITAE performance index weights the error so that the error signal converges to zero as soon as possible. The optimization objective function generates the objective function of control parameter optimization under the ITAE index, which is defined as follows:

$$fy = \sum_{t=0}^{N} L(t)|e(t)|. \tag{10}$$

Here, N is the number of search targets; $L(t)$ is the time series; and $e(t)$ is the error signal between the response frequency and the reference frequency. The smaller the Fy, the better the effect of dynamic response. As shown in Figure 6, the contents and steps of WOA are summarized.

In this paper, genetic algorithm (GA), particle swarm optimization (PSO), and whale optimization algorithm (WOA) are combined with PID and FOPID, respectively. Through different combined control strategies, the control effect of raising boring power head is further analyzed and compared. The specific parameter settings of each algorithm are shown in Table 1.

It can be seen in Table 2 for comparison of different combination strategies and control indicators, the dynamic response curve comparison diagram of each combination strategy of the regulation system is shown in Figure 7. Figure 7(a) is the step response diagram of each intelligent optimization algorithm and PID combination strategy, and Figure 7(b) is the step response diagram of each intelligent optimization algorithm and FOPID combination strategy; the comparison of PID and FOPID combined control strategies based on WOA is shown in Figure 8.

As can be seen in Figure 7, after adding PID and FOPID controllers, the system can quickly tend to a stable state. Comparing Figure 7(a) with Figure 7(b), in the control based on the same algorithm, the FOPID control is significantly better than the PID control in terms of response time and dynamic response; in Figure 7(a), the step response of WOA-FOPID control strategy is obviously better than the control strategy based on GA and PSO algorithm, and the overshoot is 8 35%, only 0.5%. Stable state is reached in 1 s; in Figure 7(b), the step response of WOA-FOPID control strategy is also better than the control strategy based on GA and PSO algorithm, at 0.5%. It reaches a stable state within 02 s, and the overshoot is only 0.5% 12137%. The simulation results in Figures 7(a) and 7(b) show that in the PID/FOPID combination strategy, the whale optimization algorithm (WOA) has more advantages than the genetic algorithm (GA) and particle swarm optimization algorithm (PSO) in the process of intelligent parameter adjustment.

Figure 8 compares the two controllers based on WOA. The results show that WOA-FOPID is more dominant, which further verifies the superiority of FOPID controller. In

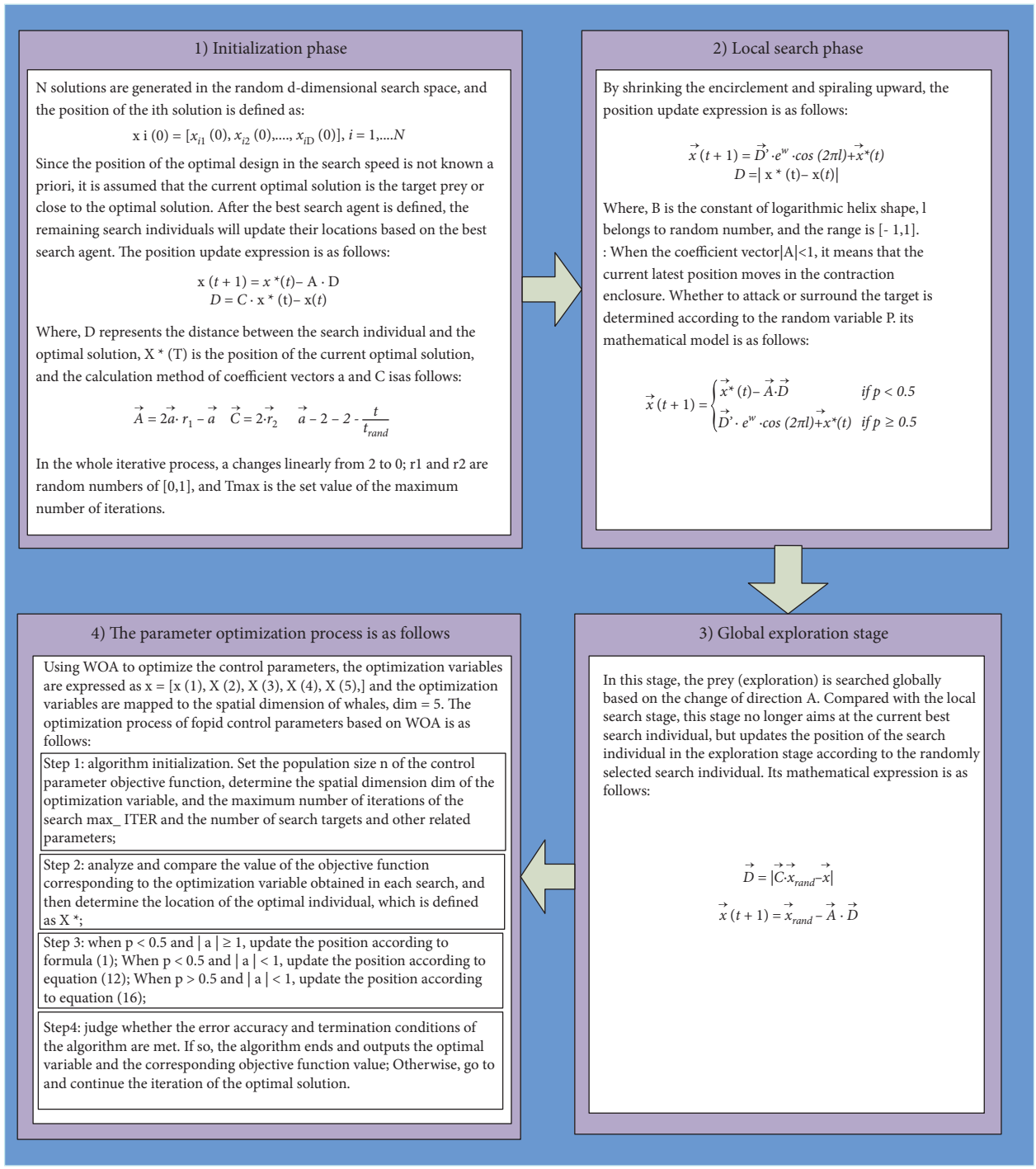

Figure 6: WOA steps and contents.

these combination strategies, it is concluded that the optimal controller is the FOPID controller based on WOA, and the parameters of the controller are as follows:

$$Gc = 15.2654 + 20s^{-1.0039} + 9.5963s^{1.1118}. \quad (11)$$

6. Experiment

To verify the correctness and effectiveness of WOA-FOPID control strategy in the electrohydraulic drive control system of the power head of raise boring machine, the performance test of the power head of raise boring machine was carried out in Liuqiao Town, Suixi County, Anhui Province. The on-site commissioning layout is shown in Figure 9.

To meet the normal operation of the rock breaking test rig, the rock breaking control system mainly adopts Siemens S7-1200 series PLC and its expansion module, combined with the control system designed by HMI to realize the start/stop action of the pump station motor, the forward/reverse action of the power head motor, the stepless speed regulation

Table 1: Specific parameter setting table of each algorithm.

	PSO	GA	WOA-FOPID	WOA-PID
Max_er	200	200	50	50
N	20	50	—	—
C1	1.49	—	—	—
C2	1.49	—	—	—
Variation parameters	—	0.8	—	—
Variation probability	—	0.75	—	—
Dim	—	—	5	3
Search agent no.	—	—	100	100

Table 2: Comparison of different combination strategies and control indicators.

Combination	Dynamic index		
	Standard variance	Overshoot (%)	Stabilization time (S)
PSO-PID	0.06309	30.1721	0.84
GA-PID	0.06309	30.1217	0.84
WOA-PID	0.03624	8.35	0.1
PSO-FOPID	0.06349	2.8197	0.51
GA-FOPID	0.03778	6.9309	0.16
WOA-FOPID	0.03535	0.12137	0.02

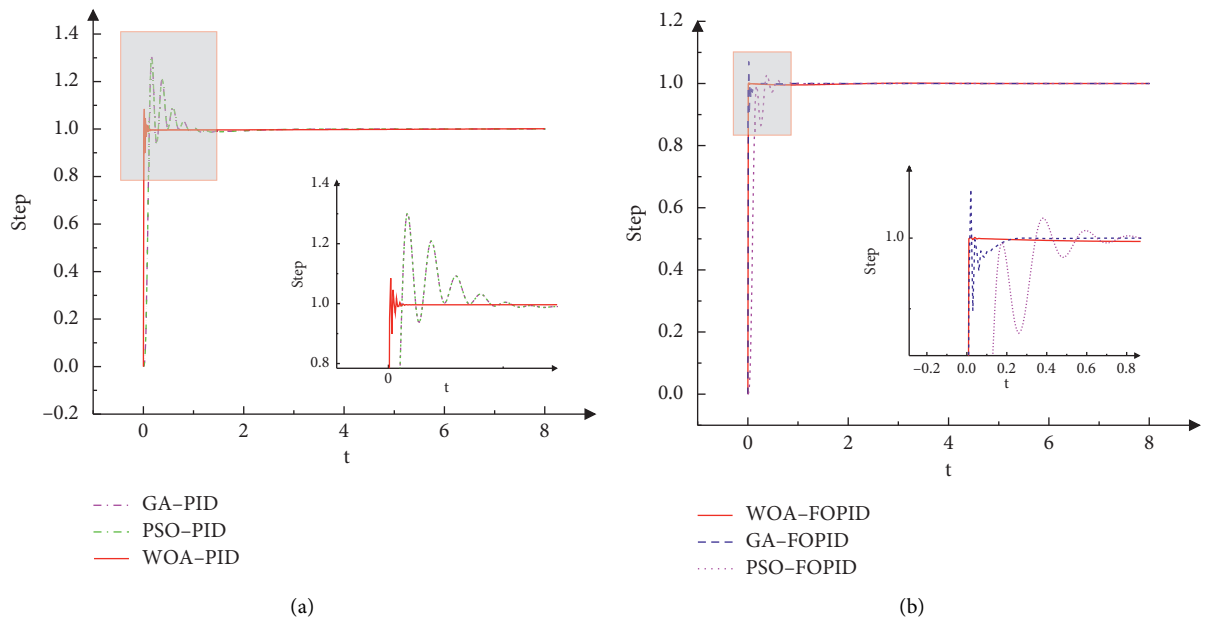

Figure 7: Comparison of dynamic response curves of each combination strategy of regulation system. (a) PID combination strategy. (b) FOPID combination strategy.

of the power head output shaft, the lifting/lowering action of the thrust cylinder, the pressure, displacement, stroke, constant pressure/constant torque drilling mode switching precise control of temperature control, and automatic operation of pump station. At the same time, the rock breaking control system is equipped with a remote control function to facilitate remote operation. S7-1200 series PLC and large screen display form the control core in the control cabinet, and each working condition monitoring and input/output drive unit cooperates with each other to ensure the stable operation of various control functions of the system. The general scheme of electric control system of raise boring machine is shown in Figure 10.

6.1. Power Head Speed Control Scheme. Power head speed regulation control model in the process of power head speed adjustment potentiometer from minimum to maximum adjusts the displacement of variable pump from 0 to 145 ml/R and variable motor from 215 to 65 ml/R in turn. That is, in the first half of the speed regulation process, the displacement of the motor remains unchanged, and only the

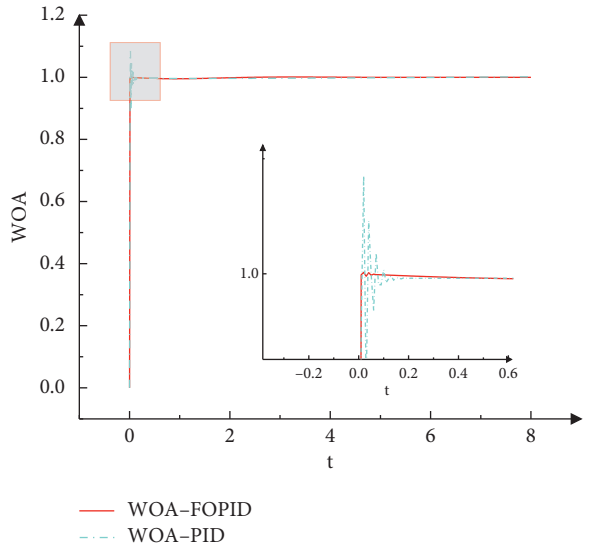

Figure 8: Comparison of control strategies based on WOA.

Figure 9: Site layout.

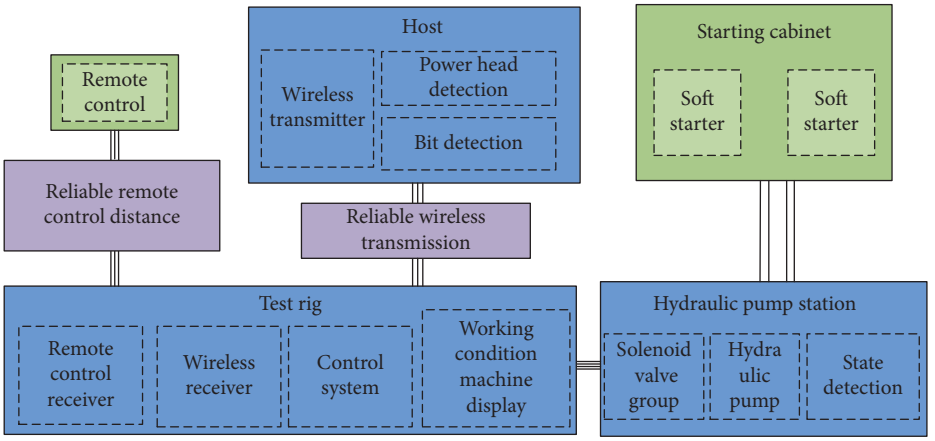

Figure 10: General scheme of the electric control system for raise boring rig.

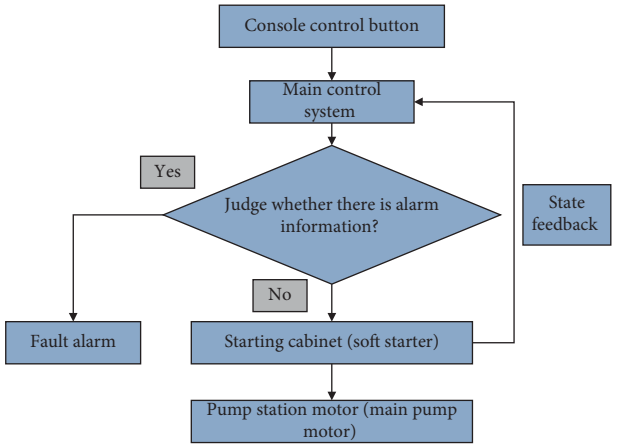

Figure 11: Control flow diagram of the main pump motor.

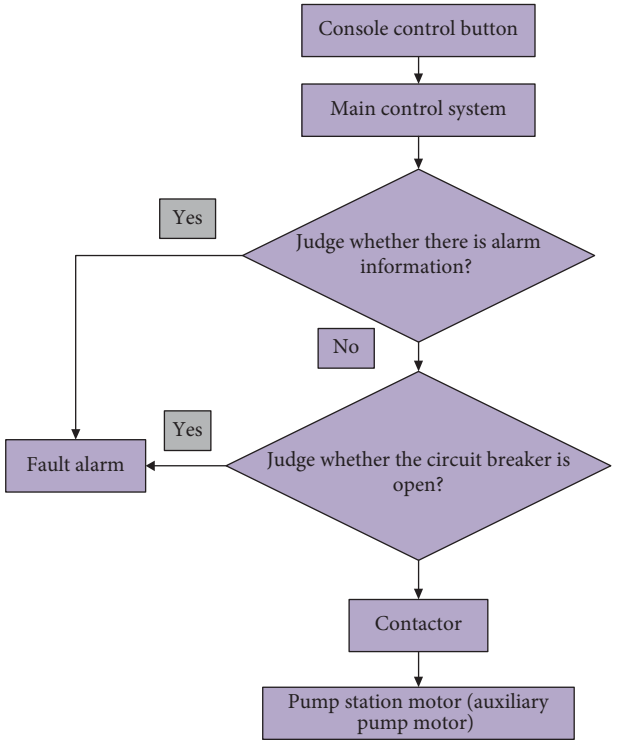

Figure 12: Control flow diagram of the auxiliary pump motor.

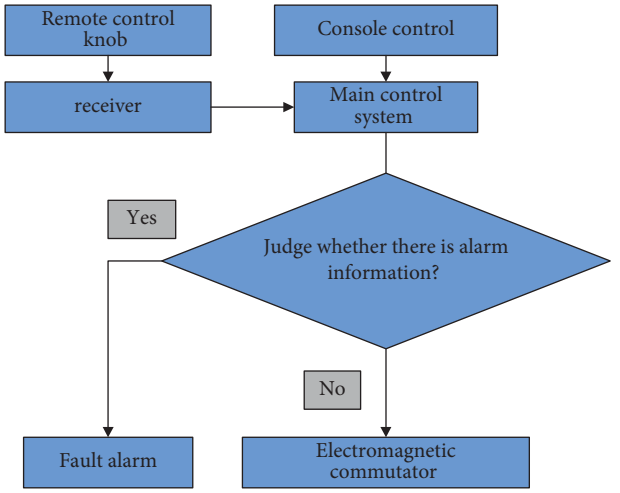

Figure 13: Flow chart of forward/reverse control of the power head.

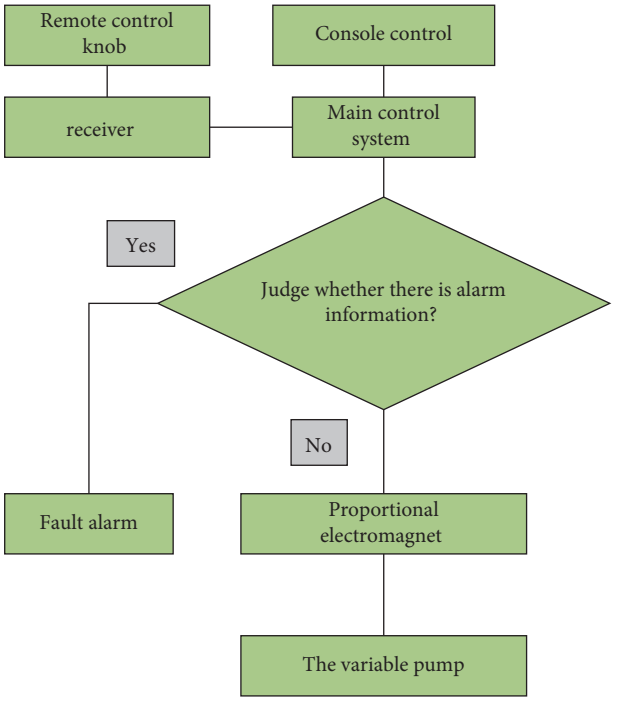

Figure 14: Flow chart of stepless speed regulation control of power head output shaft.

displacement of the variable pump is adjusted to meet the requirements of speed adjustment. In the second half, the maximum displacement output of the variable pump is maintained, and only the displacement of the variable motor is adjusted to meet the requirements of speed adjustment. In this way, no matter at any speed, the output torque is the maximum torque corresponding to the speed:

(1) *Remote Control and Valve Group Control of Hydraulic Pump Station.* Before the remote control of hydraulic pump station operates the control system, the pump station motor must be started first to make the pump station in working state. To avoid starting the pump station in another place, the system adds the start and stop button of the pump station motor on the control cabinet, and the start signal sent by the button acts on the soft starter remotely to realize the start and stop function of remote control motor.

Control Scheme. The main pump motor is started by soft starter, and the start/stop signal of soft starter is controlled through the console button to realize the start/stop control function of corresponding motor. Control process is in Figures 11 and 12.

The valve group control system sends the control command to PLC through the knob on the operation panel or the virtual button on HMI, and the output

Table 3: Experimental parameters (relationship between displacement and current of the power head motor).

Serial number	1	2
Electric current	200	600
Company	mA	mA
Displacement	216.5	0
Company	ml/r	ml/r
Maximum speed	2900	5500
Company	r/min	r/min

Table 4: Experimental parameters (relationship between pump displacement and current).

Serial number	1	2
Electric current	200	600
Company	mA	mA
Displacement	145	0
Company	ml/r	ml/r
Maximum speed	1450	1450
Company	r/min	r/min

Table 5: Experimental parameters (electromagnet at technical data EP1 and EP2).

Technical data electromagnets at EP1 and EP2			
Voltage		EP112 V (±20%)	EP212 V (±20%)
Control current (mA)	Initial control value at displacement $V_g$min	400	200
	Control termination value at displacement V_g max	1200	600

signal drives the corresponding solenoid valve action through the relay to realize the corresponding functions.

(2) The power head is driven by 160 ml/R variable pump and variable motor. To realize the adjustable steering and speed, the system designs a three-position knob to control the action of the electromagnetic directional valve, so as to realize the steering control of the power head. At the same time, the potentiometer is designed to input 0~5 V analog signal, and then, through the calculation of PLC speed regulation model, the first conductive signal of 0~10 V driving proportional amplifier is output, the proportional amplifier to output 200~600 mA current is controlled, and then the speed of power head is controlled.

Forward/Reverse Control Scheme of Power Head. Forward/reverse switching control is realized through three-position four-way solenoid directional valve. That is, the control of the electromagnetic directional valve is realized through the console knob or the remote controller knob, to realize the control of the forward/reverse switching function. Control flow is shown in Figure 13.

Stepless Speed Regulation Control Scheme of Power Head Output Shaft. The flow is adjusted by controlling the swing angle of variable pump, to realize the function of stepless speed regulation of power head output shaft. That is, the proportional electromagnet is controlled by the knob potentiometer, and then, the swing angle of the variable pump is controlled to realize the function of stepless speed regulation of the output shaft of the power head. Control flow is shown in Figure 14.

6.2. Implementation Plan. Field commissioning stage: This stage involves speed regulation of power head under shunt state. The experimental parameters are shown in Tables 3–5:

(1) Stage I: the displacement of the power head motor is kept unchanged, and the displacement of the hydraulic pump is adjusted from 0 ~ 145 (ml/r). At this time, the driving current of the power head motor is about 43 mA (the corresponding digital quantity is 2000). According to the driving characteristic curve, the maximum displacement of the power head motor is 216.5 ml/r.

(2) Stage II: the displacement of the power head motor is kept unchanged, the discharge of the hydraulic pump is adjusted to the maximum value of 145 ml/r (theoretical value), the actual control driving current is about 586 mA (corresponding to the digital quantity of 27000), and the flow of the corresponding pump is 140 ml/r. At this time, the displacement of the power head motor remains at the maximum value of 216.5 ml/r.

(3) Stage III: the maximum displacement of the hydraulic pump is kept unchanged at 145 ml/r, and the displacement of the power head motor is adjusted from 216.5 ml/r to $V_g$min. When the software controls the minimum displacement of the power head motor, the corresponding driving current is

Table 6: Meaning of each character in the text.

Symbol	Parameter meaning	Parameter value or unit
C_d	Flow coefficient of solenoid proportional directional valve	—
ρ	Hydraulic oil density	kg/m^3
A	Area of solenoid proportional directional valve port	m^2
p_s	Outlet oil supply pressure	MPa
x	Spool displacement of solenoid proportional directional valve	m
p_L	Outlet flow or load flow of solenoid proportional directional valve	m^3/s
C_{tm}	Total leakage coefficient of hydraulic motor	$C_{tm} = C_{im} + C_{em}/2$
V_t	Total volume of oil inlet chamber, oil return chamber, and connecting pipe of hydraulic motor	—
β_e	Effective bulk modulus of elasticity	—
D_m	Volume displacement per radian of hydraulic motor	—
θ_m	Angular displacement of output shaft of hydraulic motor	—
J_e	Equivalent inertia of reducer	—
B_e	Equivalent damping coefficient of reducer	—
U	Input voltage	—
F_d	Wire coil	—
i	Current in coil	—
R_c	Coil internal resistance	—
c	Damping coefficient of valve core armature assembly	—
r_p	Internal resistance of amplifier	—
K_I	Voltage force gain of proportional electromagnet	—
m	Quality of valve core armature assembly	—
L	Displacement of valve core	—
k_s	Spring stiffness of armature assembly	—
F_M	Current magnet driving force	—

about 526 mA, $V_g$min is 0.185 times, and V_g max = 216.5 ml/r × 0.185 = 40.0525 ml/r.

(4) Stage IV: the rotating speed of the power head is the maximum, and the Baote remains unchanged.

6.3. Empirical Conclusion

① Compared with "the power head parameter table of enhanced TD2000 drilling rig under shunting state and turning into working condition," there is an error in the maximum displacement control of hydraulic pump station, with an error of about 5 ml/r. There is still a little room for optimization, which can be optimized on-site.

② Compared with "the power head parameter table of enhanced TD2000 drilling rig under shunting condition and turning into working condition," the minimum displacement control of power head motor has error, and the error is about 2 ml/r, so the optimization needs to be careful (during plant commissioning, when the speed regulation exceeds a certain position, the speed of power head decreases instead).

③ In the whole speed regulation process, the trend is basically consistent with the table of power head parameters under shunting condition of enhanced TD2000 drilling rig, but there is a little error at the two end points. The error is as described in points ① and ② above. The position number described in the table is included in the whole speed regulation process and does not need to be corrected separately. Only the corresponding speed identification needs to be carried out on-site. The corresponding position is marked.

7. Conclusion

Aiming at the problem of whether the power head of raise boring machine can be driven in complex environment during reaming operation, using the fine-tuning characteristics of FOPID control to apply to the nonlinear control object, a method of adjusting FOPID control parameters based on whale optimization algorithm (WOA) is proposed. Through the establishment of the electrohydraulic coupling model of the power head of the raise boring machine and the simulation analysis in MATLAB software, the following conclusions are obtained (Table 6):

(1) From the simulation results of six different combined control strategies, it can be seen that the overall control effect of FOPID is much better than PID control in the overshoot and response time in the frequency response curve. In PID control, the overshoot is at least 8.35%, while the overshoot of FOPID control is at most 6.9309%. The results show that FOPID is more suitable for the electrohydraulic control of raising boring than PID, and the overall response time is shorter. It can adjust the angular speed of the power head in time and then control the fast and slow switching of the power head, which shows that FOPID control has a better application prospect in the electrohydraulic drive control of raising boring.

(2) Among the six combined control strategies, the combined strategy based on WOA has obvious

advantages in each control method. The overshoot of WOA-PID control strategy in PID control is at least 8.35% and takes 0.1 s; the overshoot of WOA-FOPID control strategy in FOPID control is at least 0.12137%, with a time of 0.02 s. From the numerical iteration process of WOA objective function, it can be found that WOA has good optimization ability and convergence performance, which verifies the excellent performance of WOA in control parameter tuning. The experimental data show that the WOA-FOPID combined control strategy studied in this paper can respond to the input in time, and the FOPID parameters are adjusted through WOA, which has a good effect on the optimization of control parameters and can effectively improve the control accuracy of FOPID.

(3) After the design of the control system is completed, it is debugged and applied on the raise boring rig. The control system realizes various functions including remote pump station start and stop control and single/double drive motor switching control and meets the requirements of process operation. Experiments show that the WOA-FOPID control strategy is effective in the electrohydraulic drive control system. The control strategy can make the electrohydraulic drive control have good real time, accuracy, and rapidity and can realize fast power head. Slow switching and high-precision control can be used as the exclusive control system of raise boring rig.

Data Availability

The dataset can be accessed upon request to the corresponding author.

Disclosure

An earlier version of this paper has been presented as preprint according to the following link: https://www.researchsquare.com/article/rs-1500559/v1 [39].

Conflicts of Interest

The authors declare that they have no conflicts of interest.

Authors' Contributions

Jun Zhang designed the overall research scheme, programmed and debugged the algorithm, and wrote the paper. Qinghua Liu, Yun Chen, and Jiguo Wang debugged the algorithm. Jinpu Feng, Qingliang Meng, and Wei Cao programmed the algorithm. Wei Tu and Xiaohui Gao checked the language of the paper.

Acknowledgments

The authors thank Youth Fund of National Natural Science Foundation of China, project name: research on uncertain motion characteristics and compound control mechanism of drilling and anchor manipulator based on Chebyshev interval algorithm, No. 52104165; Free Exploration General Fund of Shanxi Provincial Department of Science and Technology, project name: motion uncertainty analysis and closed-loop feedback control mechanism of drilling anchor manipulator, No. 20210302123123; and State Key Laboratory of Robotics and Systems, project name: research on motion uncertainty characteristics and compound control mechanism of manipulator of anchor drilling robot, No. SKLRS-2021-KF-16.

References

[1] H. Wang, "Hydraulic system design of raise boring machine using cartridge valve," *Mechanical design and manufacturing engineering*, vol. 48, no. 7, pp. 71–73, 2019.

[2] W. Shen and S. Liu, "Adaptive robust integral control of hydraulic motor servo position system based on network," *Journal of Shanghai University of technology*, vol. 43, no. 04, pp. 325–331, 2021.

[3] Y. Yang, *Research on Control Algorithm of Electro-Hydraulic Proportional Valve Controlled Four cylinder Synchronization*, Lanzhou University of technology, Lanzhou, China, 2019.

[4] L. Cheng, *Design and Research on Electro-Hydraulic Control System of Rotary Steering Drilling Tool Test Bench*, Xi'an University of petroleum, Xi'An, China, 2021.

[5] Y. Zhang, *Research On Key Technology of Performance Optimization of Electromechanical Hydraulic Integrated System of Drilling Rig*, General Coal Research Institute.

[6] X. Tong Research, *On Hydraulic Drive and Control System of Shield Cutterhead*, Zhejiang University, Zhejiang, China, 2008.

[7] L. Li, B. Lei, and C. Mao, "Digital twin in smart manufacturing," *Journal of Industrial Information Integration*, vol. 26, no. 9, Article ID 100289, 2022.

[8] D. Xue, "Zhao chunna design of fractional order PID controller for fractional order system," *Control theory and application*, no. 05, pp. 771–776, 2007.

[9] L. Li and C. Mao, "Big data supported PSS evaluation decision in service-oriented manufacturing," *IEEE Access*, vol. 8, no. 99, pp. 154663–154670, 2020.

[10] L. Li, T. Qu, Y. Liu et al., "Sustainability assessment of intelligent manufacturing supported by digital twin," *IEEE Access*, vol. 8, pp. 174988–175008, 2020.

[11] C. Yuan, J. Cai, and X. Wang, "Research on PID controller of vehicle suspension based on particle swarm optimization algorithm," *China Journal of agricultural machinery chemistry*, vol. 25, no. 5, p. 7, 2019.

[12] L. Li, C. Mao, H. Sun, Y. Yuan, and B. Lei, "Digital twin driven green performance evaluation methodology of intelligent manufacturing: hybrid model based on fuzzy rough-sets AHP, multistage weight synthesis, and PROMETHEE II," *Complexity*, vol. 2020, no. 6, pp. 1–24, 2020.

[13] J. Meng, H. Yang, and Q. Chen, "Simulation Research on PID control of automotive semi-active suspension based on genetic algorithm optimization," *Modern manufacturing engineering*, no. 6, p. 5, 2013.

[14] G. Wen, Xu Gong, Z. Li, and Z. Zhou, "Static output feedback control of vehicle semi-active suspension based on ILMI algorithm," *Automotive Engineering*, vol. 29, no. 6, p. 4, 2007.

[15] D. Xue, *Fractional Calculus and Fractional Control*, Science Press, Beijing, China, 2018.

[16] Z. Liu, C. song, S. Cheng et al., "Development history and current situation of drilling technology and equipment of raise boring rig in China," *Coal science and technology*, vol. 49, no. 01, pp. 32–65, 2021.

[17] F. Jingpu, C. Yun, K. Ma, and kuiwu Xu, "Tu Wei Design of electric control system for td2000/1200 top drive drilling rig," *Coal mining machinery*, vol. 42, no. 8, pp. 18–21, 2021.

[18] S. Mirjalili and A. Lewis, "The whale optimization algorithm," *Advances in Engineering Software*, vol. 95, no. 95, pp. 51–67, 2016.

[19] R. Li, B. Jc, C. Cx, and R. Manivannand, "Quasi-stability and quasi-synchronization control of quaternion-valued fractional-order discrete-time memristive neural networks," *Applied Mathematics and Computation*, vol. 395, Article ID 125851.

[20] M. Dalir and N. Bigdeli, "The design of a new hybrid controller for fractional-order uncertain chaotic systems with unknown time-varying delays," *Applied Soft Computing*, vol. 87, Article ID 106000.

[21] B. Sdna, D. Bao, and C. Sbc, "Smart dampers-based vibration control – Part 2: fractional-order sliding control for vehicle suspension system," *Mechanical Systems and Signal Processing*, vol. 148.

[22] S. Bushnaq, T. Saeed, D. Torres, and Z. Anwar, "Control of COVID-19 Dynamics through a Fractional-Order model," *Alexandria Engineering Journal*, vol. 60, no. 4, pp. 3587–3592, 2021.

[23] M. N. Musarrat and A. Fekih, "A fractional order sliding mode control-based topology to improve the transient stability of wind energy systems," *International Journal of Electrical Power & Energy Systems*, vol. 133, no. 107306, pp. 107306–107312, 2021.

[24] I. Podlubny, "Fractional-order systems and PI/sup/spl lambda//D/sup/spl mu//-controllers $\overrightarrow{r}$ controller," *IEEE Transactions on Automatic Control*, vol. 44, no. 1, pp. 208–214, 1999.

[25] X. Wu and Y. Huang, "Adaptive fractional-order non-singular terminal sliding mode control based on fuzzy wavelet neural networks for omnidirectional mobile robot manipulator - sciencedirect," *ISA Transactions*, vol. 121, pp. 258–267, 2021.

[26] H. M. Cuong, H. Q. Dong, P. V. Trieu, and L. A. Tuan, "Adaptive fractional-order terminal sliding mode control of rubber-tired gantry cranes with uncertainties and unknown disturbances," *Mechanical Systems and Signal Processing*, vol. 154, Article ID 107601, 2021.

[27] A. Sh, W. A. Jie, H. C. Chen et al., "A fixed-time fractional-order sliding mode control strategy for power quality enhancement of PMSG wind turbine," *International Journal of Electrical Power & Energy Systems*, vol. 134, Article ID 107354, 2022.

[28] D. Chu and H. Chen, "Wang Xuguang Whale optimization algorithm based on adaptive weight and simulated annealing," *Electronic news*, vol. 47, no. 5, pp. 992–999, 2019.

[29] D. Butti, S. K. Mangipudi, and S. R. Rayapudi, "An improved whale optimization algorithm for the design of multi-machine power system stabilizer," *International Transactions on Electrical Energy Systems*, vol. 30, no. 5, 2020.

[30] J. U. N. Zhang, C. F. Wang, and L. Wang, *Intelligent Control Strategy of Electro-Hydraulic Drive System for Raising Boring Power Head*, 2022, https://www.researchsquare.com/article/rs-1500559/v1A.